

# Effect of Electrochemical Micromachining Process Parameters on Surface Roughness and Dimensional Deviation of Ti6Al4V by Tungsten Electrode



Venkatasreenivasula Reddy Perla, Subbarama Kousik Suraparaju,  
K. J. RathanRaj and A. Sreenivasulu Reddy

**Abstract** The electrochemical micromachining (ECMM) is a special form of conventional ECM process in which the tool electrode is at micro-level used to produce micro-features. This article aims to determine the parametric influence of process parameters in ECMM using Taguchi's experimental design and ANOVA. The objective variables are surface roughness (SR) and dimensional deviation (DD). Experiments were designed as per Taguchi's L16 orthogonal array (OA) by considering applied voltage (V), duty cycle (DC), feed rate ( $F$ ) and frequency ( $f$ ) as input parameters. Experiments carried on Ti6Al4V using sodium chloride (NaCl) salt solution with concentration 20 g/lit by producing blind holes of depth 250  $\mu\text{m}$ . Surface roughness is measured with non-contact surface roughness tester Talysurf CCI (coherence correlation interferometry) having  $< 0.01$  nm as least count and dimensional deviation is measured with vision measuring machine. ANOVA technique is performed to get percentage influence of each process parameter on performance characteristics, and it is observed that duty cycle has more influence on surface roughness and applied voltage has more influence on dimensional deviation.

**Keywords** Electrochemical micromachining · Electrolyte · Tungsten tool · Taguchi L16 OA · ANOVA

---

V. R. Perla (✉) · S. K. Suraparaju · A. Sreenivasulu Reddy  
Mechanical Engineering Department, Sri Venkateswara University, Tirupati, Andhra Pradesh,  
India  
e-mail: [perlasreenu@gmail.com](mailto:perlasreenu@gmail.com)

V. R. Perla · K. J. RathanRaj  
Industrial Engineering and Management Department, B.M.S. College of Engineering, Bengaluru,  
Karnataka, India

S. K. Suraparaju  
Department of Mechanical Engineering, National Institute of Technology Puducherry, Karaikal,  
Ut of Puducherry, India

# 1 Introduction

The significant electrochemical machining (ECM) was developed during 1959, and it is mainly operated for materials that are hard to machine with conventional machining operations. Electrochemical micromachining (ECMM) is an application of ECM for a precise shape in the micromachining range, in which micromachining is the component machining in dimension ranging between 1 and 999  $\mu\text{m}$  [1, 2]. Micro-machining is directly not possible to achieve by a conventional technique because micron-dimensional accuracies are involved in it.

The exigency towards the use of more micro-parts is demanded due to drastic changes in the utilization of various industrial components. For example, fuel injection nozzle design is changed according to environmental constraints and made it more compact with high accuracy. ECCM is best suited for this high-end usage of micro-parts, due to its various advantages such as higher machining rate, machining a wide range of materials, better precision and control, economical and also it is environmentally friendly. This method can effectively process the electrically conductive, hard and difficult to machine materials without any defects and deformation. During machining, there is no residual stresses development and no tool wear problem because there is no direct contact between tool electrode and workpiece. Since the electrolysis principle is the cause for mechanism of material removal, there is no heat generation during the process. These capabilities and qualities of ECMM make it useful in many industries where difficult-to-cut materials are to be processed [3–7] (Fig. 1).

The miniaturization components in various applications through the micromachining process are the current trend in machining. Micromachining is the key technology in microelectromechanical systems (MEMS). This technology lasts long and

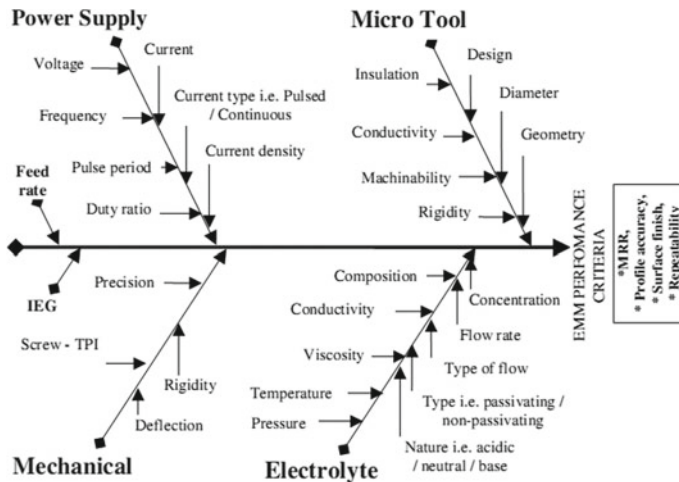


Fig. 1 Fishbone diagram of electrochemical micromachining (ECMM) [19]

will be more effective due to its effective space utilization, and also it has high accuracy and efficacy. ECMM can be operated in maximum applications associated with the micromachining due to its economic efficacy and the achievable high precision [8–11]. The process variables like applied machining voltage (V), duty cycle (%), feed rate ( $\mu\text{m}$ ) and frequency (Hz) influence the surface roughness of the machined component. These parameters are to be optimized in such a way that the machined surface has an acceptable surface roughness. The surface roughness of this hole is measured by a highly precise instrument with minimum least count and also by a non-contact method such as light interferometry [12–15]. In recent years, a double-pulsed wire electrochemical micromachining is developed to cut profiles on the workpiece electrode like wire electrical discharge machining and also improve the stability in machining [16, 17]. Advanced engineering materials like bulk metallic glasses are also processed using ECMM [18].

## 2 Experimental Details

### 2.1 Experimental Set-up

The set-up employed for micro-hole drilling (500  $\mu\text{m}$  diameter) is shown in the Fig. 2. This set-up comprises power supply system, electrolytic system, tool holding arrangement, controller unit, working platform and machining chamber. Experiments were conducted using NaCl (20 gm/l) as an electrolyte. Machining chamber is comprised of a work holding device, an LED light and a blow-off system. Even though there is a provision for the electrolyte flow in the set-up, in order to perform the vibration-less and smooth experimentation (to reduce tool vibration due to electrolyte pressure), die-sinking-type electrochemical machining is performed in this investigation. ECMM provides a smaller inter-electrode gap (IEG) without electrolyte boiling in the gap ranging from 10 to 80  $\mu\text{m}$  which requires limiting the IEG valve across tool and workpiece. Model experiments performed to fix the inter-electrode gap, and it is fixed as 25  $\mu\text{m}$ . The short-circuiting between workpiece and tool has occurred for the IEG which is smaller than the 25  $\mu\text{m}$ . For smaller IEG, i.e. less than 25  $\mu\text{m}$ , there is a chance of short-circuiting which causes defective machined surfaces.

ECMM experimental set-up works with the pulsed power supply of rectangular pulsed shape with a controller monitor connected to it. Since it is a pulsed power supply, pulse on time and pulse off time are the major electrical parameters along with applied current and voltage. The current and voltage indicators are shown in orange and yellow colours when the machining is performed and current is adjusted by the machine automatically based on the machining feed rate and other machining conditions, whereas voltage can be manually changeable. The other important parameter in ECMM is feed rate; it can be varied by using the controller through machine attached monitor and the input is given in the range of  $\mu\text{m/s}$ . The work platform is a plastic rectangular vessel having work holding platform with strong

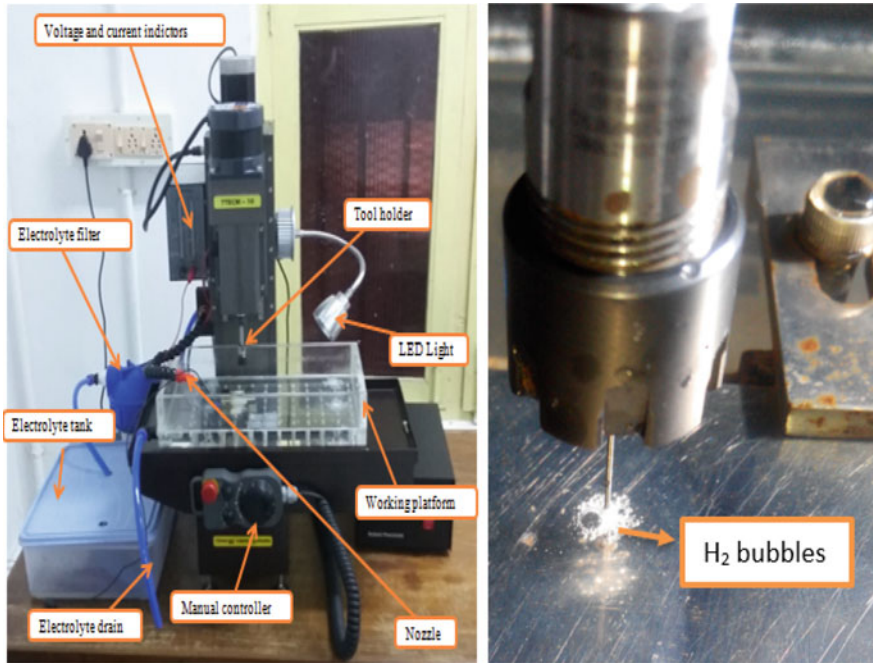


Fig. 2 ECMM experimental set-up and tool holder arrangement

magnets above and below the holder which holds the electrode during the machining without any movement. Along with this, electrolyte flowing system is attached to tank, filter, nozzle and recirculation system. A manual control is provided for giving instructions to the working platform and movement of tool holder in X-Y-Z directions.

### 2.2 Experimental Design

In the current study, an experimental study has been performed to find out the parametric influence on the output responses of the ECMM method. Due to its inherent properties and importance in manufacturing and aerospace industries, the titanium alloy (Ti6Al4V) of 100 mm X 60mm X 0.9mm is selected and employed as workpiece in the current study.

### 2.2.1 Selecting Factors and Factor Levels

The Taguchi method is an effective technique for designing and conducting experiments in various effective manufacturing systems because of its simplicity and applicability for producing robust designs. Taguchi technique gives the least number of experimental runs to be carried out for yielding optimum results. In order to fix a relation between the input parameters and output responses, an extensive information was collected on machine capability, available limits in the machine parameters along with the previous records and literature surveys. Thus, four variables chosen for experimental design are applied voltage (V), duty cycle (%), feed rate ( $\mu\text{m}$ ) and frequency (Hz). From the collected data, four levels are selected for each parameter and thus the design is made by the combination of four parameters and four levels. The input parameters and their levels are shown in Table 1. Duty cycle and frequency are determined by using the following formulas:

$$T_{\text{total}} = T_{\text{on}} + T_{\text{off}}$$

$$\text{Duty cycle} = \frac{T_{\text{on}}}{T_{\text{total}}}$$

$$\text{frequency} = \frac{1}{T_{\text{total}}}.$$

### 2.3 Machining of Titanium Alloys

Titanium alloys are known for the better bio—compatibility and having a wide range of applications in the medical field like surgical instruments, bone implants, tooth implants and knee implants, etc. All these mentioned applications are shaped out with the operation of micro machining process for better viability. The micromachining of titanium and titanium alloys particularly in electrochemical micromachining (ECMM) is different when compared with any other commonly used metals. Titanium alloys have a tendency to develop thin tenacious film of oxide when it is exposed

**Table 1** Levels and actual values of input parameters in ECMM

| S. No. | Input parameter               | Level 1 | Level 2 | Level 3 | Level 4 |
|--------|-------------------------------|---------|---------|---------|---------|
| 1      | Applied voltage (V)           | 12      | 14      | 16      | 18      |
| 2      | Duty cycle (%)                | 20      | 40      | 60      | 80      |
| 3      | Feed rate ( $\mu\text{m/s}$ ) | 0.3     | 0.6     | 0.9     | 1.2     |
| 4      | Frequency (Hz)                | 30      | 40      | 50      | 60      |

to the surrounding containing oxygen. Because of this developed oxide layer, machining of titanium alloy is very difficult. During electrolysis to dissolve the titanium metal atoms into titanium ions, higher voltages are required when compared to other materials. The authors have performed some trial experiments within the range 5–25 V machining voltage with combination of various machining parameters viz. electrolyte concentration, duty cycle, frequency and tool feed rate. From the data of trial experiments, it has been revealed that the machining can only be possible normally at machining voltages 10–20 V. The selection of suitable electrolyte and its concentration is another deciding factor for machining of titanium alloys. In the present work, the saltwater containing sodium chloride with 20 grams per litre is used. The accuracy and precision of the final machined component in ECMM are highly influenced by the process parameters viz. applied voltage, pulse duty cycle, tool feedrate and frequency. Therefore, in achieving the desired results during machining of titanium alloys proper selection and controlling of these parameters play an important role.

### 2.3.1 Electrolysis

Electrolysis is the process in which electric current is used to make chemical changes in any electrically conducting substance. In ECMM, workpiece is connected to a positive terminal of power supply and tool is connected to a negative power supply. Electrolyte used in this experimentation (NaCl electrolyte) conducts electricity, and the current is carried by the atoms (group of atoms) of electrolyte not by the electrons. These atoms are going to lose or gain electrons by obtaining either negative or positive charges and also known as ions. The ions having negative charge are attracted by anode, and they moved through the electrolyte in the direction of negative current and named as anions. Similarly, the positively charged ions attracted towards negative electrode (cathode) and these are referred as cations. As the potential difference applied, due to electrolysis the water is dissociated into hydrogen and hydroxide ions and electrolyte dissolved into both sodium ions and chloride ions.

The free electrons are gained by the hydrogen ion to become hydrogen gas and liberated at cathode during machining as shown in Fig. 2. The metal ions at anode are also participated in the chemical reaction to form respective metal hydroxide precipitations. Along with this, sodium hydroxide and metal chlorides also formed since the amount of chlorine and aluminium and vanadium very small amount of these products are resulted. If the pulse off time is very small then the available electrolyte to remove the sludge is very small and it results in improper machining surface. All the chemicals used in the research are shown below (Figs. 3 and 4).

### 2.3.2 Chemical Reactions

As the applied potential difference reaches breakdown, electrolysis comes into action and the electrolyte dissociates water and NaCl as follows:

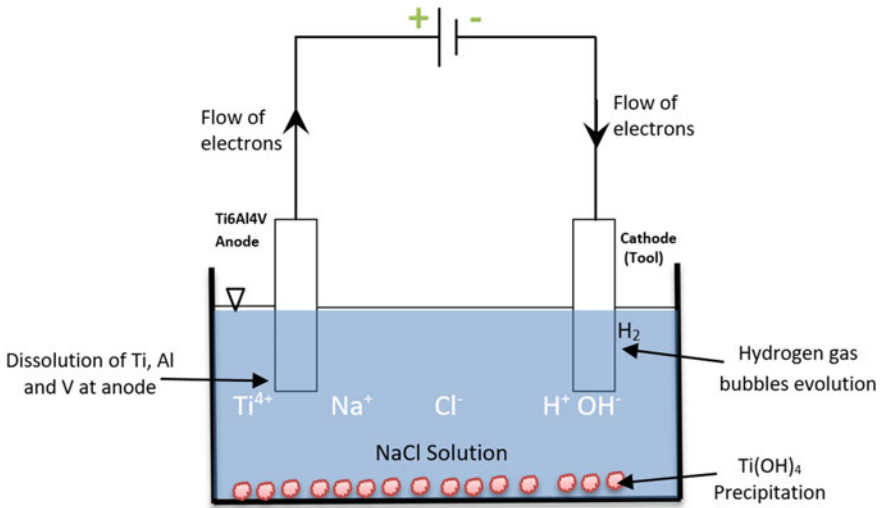
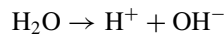
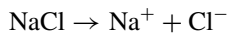


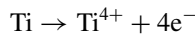
Fig. 3 Electrolysis of titanium alloy with NaCl electrolyte

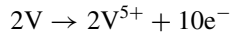


Fig. 4 NaCl electrolyte before and after machining



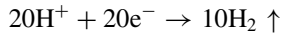
At anode, the metal atoms become metal ions by losing electrons.  
 Reactions at anode:



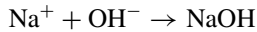
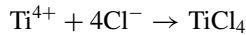
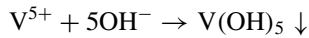
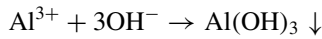
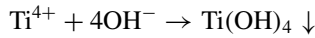


By gaining the free electrons from anode, hydrogen ions are converted to hydrogen gas and appeared as bubbles.

Reactions at cathode:



The outcome of the electrochemical reaction is that the combination with other ions to precipitate as metal hydroxides and little bit chlorides



Since the percentage of aluminium (Al) and vanadium (V) is very less, the products formed from these elements like  $\text{Al}(\text{OH})_3$ ,  $\text{V}(\text{OH})_5$  are also very small in amount.

## 2.4 Output Parameters

The output parameters considered for this study are dimensional deviation and surface roughness. Dimensional deviation is measured with the help of vision measuring machine by measuring the diameter of the hole on the topmost surface of the work-piece material. This diameter is calculated by considering 6–8 points on the periphery of the hole, and according to the suggestions, machine covers all the points with a diameter value. Dimensional deviation is determined with the following formula.

$$\text{Dimensional Deviation} = \frac{D_h - D_t}{2}$$



where

$D_h$  Diameter of the hole at top surface of the workpiece;

$D_t$  Diameter of the tool 500  $\mu\text{m}$ .

Surface roughness is measured with non-contact surface roughness tester (Talysurf-CCI). To determine surface roughness value, blind holes are performed with 250  $\mu\text{m}$  as the depth of the hole. The surface roughness tester works with coherence correlation interferometry principle. The white light beam produced by the optical fibre is supplied to the equipment. The white light beam passes through a beam splitter, which splits the beam into two parallel splits. One split of the beam is reflected towards the target sample, while the second passes towards an internal reference mirror. Both beams again combine and give a local interference image; this is directed towards charge-coupled device detector (CCD). The microscope has optical measuring head which is coupled to piezoelectric actuators (PZT). Location of different points on the sample surface is found out using the analysis of mutual temporal coherence of interfering waves, which are applied individually to each surface point. The monitor connected to the equipment generates surface topography. Based on the magnification of the instrument, the number data points to be check is determined [16–19]. The equipment sample reading contains 2D and 3D and advanced 3D views and waviness graphs of surface profiles in pseudo-colours. With the help of surface profile and topography, all surface parameters ( $R_p$ ,  $R_v$ ,  $R_z$ ,  $R_c$ ,  $R_a$  and  $R_t$ , etc.) are determined (Figs. 5, 6 and 7).

### 3 Results

The ECMM experiments are conducted with Tungsten tool of 500  $\mu\text{m}$  as diameter for titanium alloy (Ti6Al4V). In order to achieve proper circularity of machined holes, the anode tool is properly ground. The test job specimen of size 100 mm  $\times$  60 mm  $\times$  0.9 mm is prepared by using WEDM machine, and the electrolyte used for this experimental work is sodium chloride (NaCl) solution with twenty grams per litre as electrolyte concentration. Inter-electrode gap is also maintained constantly throughout the experiment (Table 2).

It can be seen from the experimental results of Ti6Al4V that the obtained dimensional deviation (DD) ranges from 156 to 477  $\mu\text{m}$  and these values are measured with vision measuring machine (VMS-10). High-dimensional deviation is due to high applied voltage and with the use of non-coating tool (electrode). The results of surface roughness are 0.142–1.260  $\mu\text{m}$ , and these readings are measured using non-contact surface roughness measuring machine (Talysurf-CCI) with the accuracy of < 0.01 nm (Tables 3 and 4).

The main effect plot for dimensional deviation shows that the major contributor for minimum dimensional deviation. From Table 5, it is applied voltage, followed by the feed rate. The increase in the applied voltage increases the current density at the machining zone. Hence, the high current density supported with voltage has

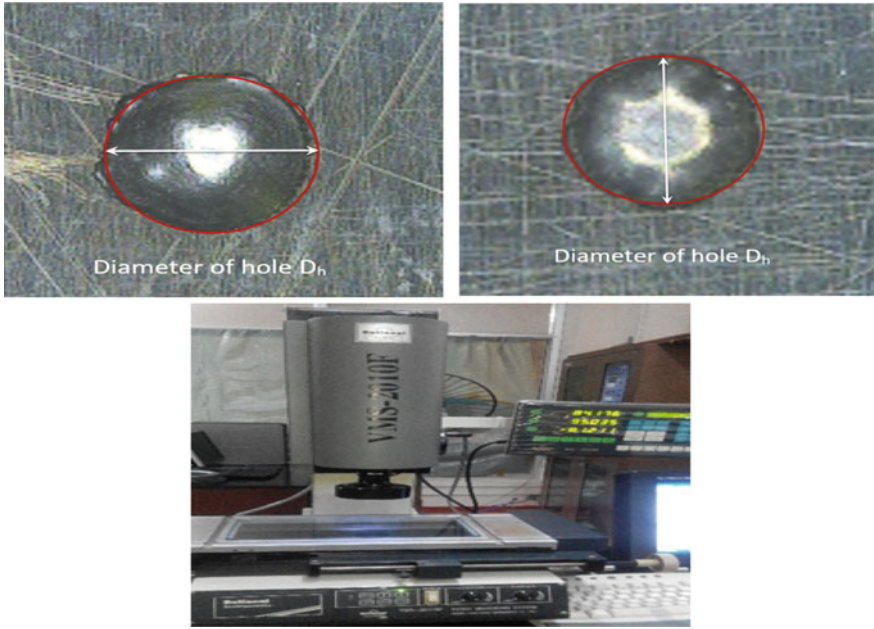


Fig. 5 Measurement of hole diameter ( $D_h$ ) by vision measuring machine (VMS)

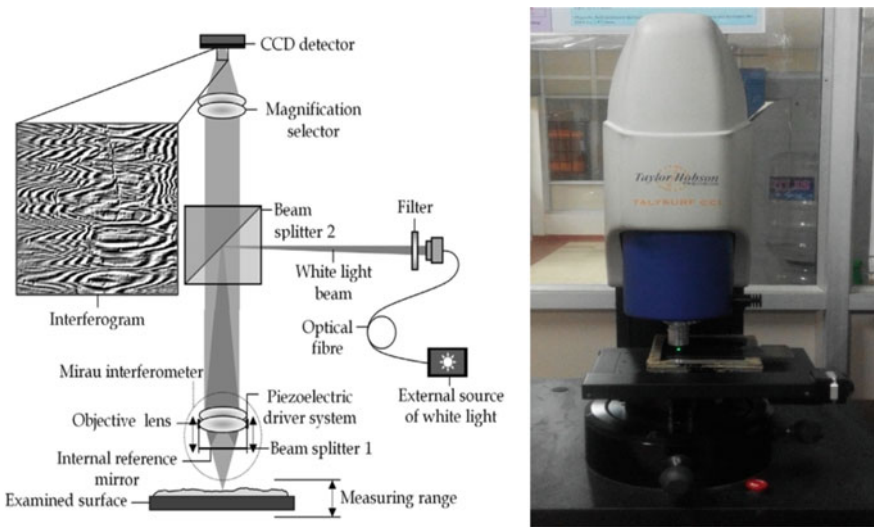
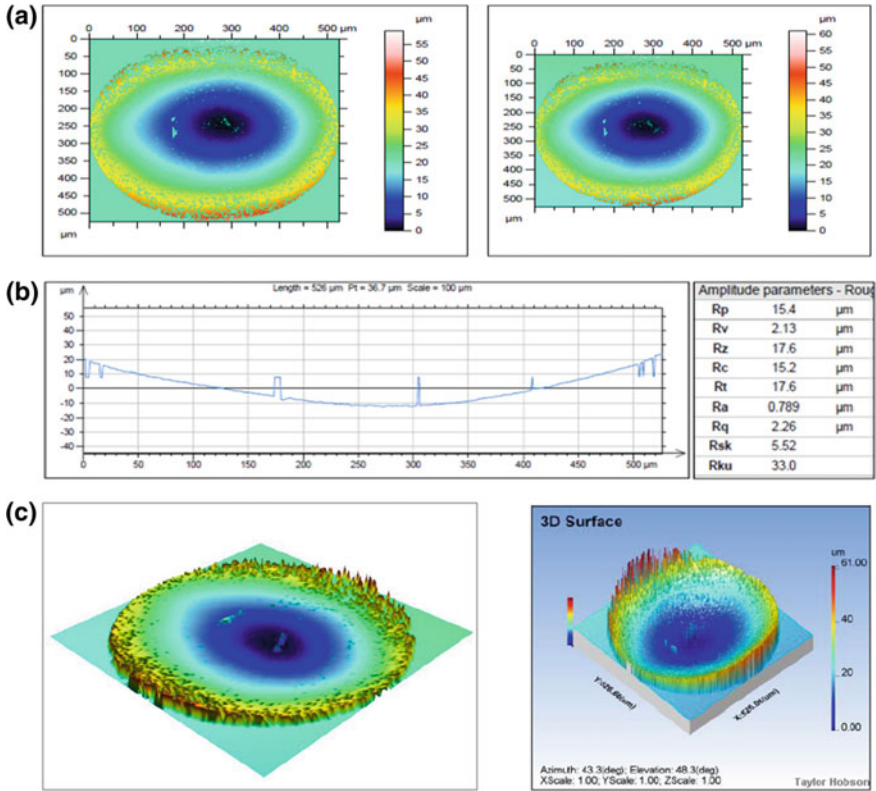


Fig. 6 Working principle of the non-contact surface roughness tester Talysurf-CCI [20]



**Fig. 7** Sample reading of non-contact surface roughness tester **a** 2D view pseudo-colour surface map, **b** surface profile with sample length and surface parameters and **c** 3D and advanced 3D views of surface topography

emerged as a major contribution to dimensional deviation for Ti6Al4V. Similarly, the main effect plot for surface roughness shows that the major contributor for minimum surface roughness is duty cycle followed by frequency of the pulse from Table 6. Due to increase in duty cycle, pulse on time increases and pulse off time reduces which results in very less time available to remove the machined debris which causes improper surface finish.

### 3.1 Results of ANOVA

See Tables 5 and 6.

**Table 2** Experimental design and output response values

| Expt. No. | Applied voltage (V) | Duty cycle (%) | Feed rate ( $\mu\text{m/s}$ ) | Frequency (Hz) | Dimensional deviation (mm) | Surface roughness ( $\mu\text{m}$ ) |
|-----------|---------------------|----------------|-------------------------------|----------------|----------------------------|-------------------------------------|
| 1         | 12                  | 20             | 0.3                           | 30             | 0.286                      | 0.820                               |
| 2         | 12                  | 40             | 0.6                           | 40             | 0.201                      | 0.142                               |
| 3         | 12                  | 60             | 0.9                           | 50             | 0.214                      | 0.615                               |
| 4         | 12                  | 80             | 1.2                           | 60             | 0.256                      | 0.789                               |
| 5         | 14                  | 20             | 0.6                           | 50             | 0.190                      | 0.230                               |
| 6         | 14                  | 40             | 0.3                           | 60             | 0.346                      | 0.208                               |
| 7         | 14                  | 60             | 1.2                           | 30             | 0.156                      | 0.882                               |
| 8         | 4                   | 80             | 0.9                           | 40             | 0.230                      | 0.775                               |
| 9         | 16                  | 20             | 0.9                           | 60             | 0.225                      | 0.176                               |
| 10        | 16                  | 40             | 1.2                           | 50             | 0.253                      | 0.834                               |
| 11        | 16                  | 60             | 0.3                           | 40             | 0.366                      | 0.143                               |
| 12        | 16                  | 80             | 0.6                           | 30             | 0.298                      | 0.461                               |
| 13        | 18                  | 20             | 1.2                           | 40             | 0.432                      | 0.215                               |
| 14        | 18                  | 40             | 0.9                           | 30             | 0.295                      | 0.155                               |
| 15        | 18                  | 60             | 0.6                           | 60             | 0.390                      | 0.198                               |
| 16        | 18                  | 80             | 0.3                           | 50             | 0.477                      | 1.260                               |

**Table 3** Response table for S/N ratios—dimensional deviation

| Level | Applied voltage (V) | Duty cycle (%) | Feed rate ( $\mu\text{m/s}$ ) | Frequency (Hz) |
|-------|---------------------|----------------|-------------------------------|----------------|
| 1     | 12.509              | 11.386         | 8.813                         | 12.032         |
| 2     | 13.137              | 11.424         | 11.764                        | 10.681         |
| 3     | 11.035              | 11.610         | 12.429                        | 11.546         |
| 4     | 8.126               | 10.386         | 11.800                        | 10.547         |
| Delta | 5.011               | 1.223          | 3.616                         | 1.485          |
| Rank  | <b>1</b>            | <b>4</b>       | <b>2</b>                      | <b>3</b>       |

**Table 4** Response table for S/N ratios—surface roughness

| Level | Applied voltage (V) | Duty cycle (%) | Feed rate ( $\mu\text{m/s}$ ) | Frequency (Hz) |
|-------|---------------------|----------------|-------------------------------|----------------|
| 1     | 6.240               | 10.733         | 7.562                         | 6.433          |
| 2     | 7.427               | 12.091         | 12.628                        | 12.353         |
| 3     | 10.071              | 9.068          | 9.430                         | 4.139          |
| 4     | 10.401              | 2.248          | 4.519                         | 11.213         |
| Delta | 4.161               | 9.843          | 8.109                         | 8.214          |
| Rank  | <b>4</b>            | <b>1</b>       | <b>3</b>                      | <b>2</b>       |

**Table 5** ANOVA for dimensional deviation

| Source                        | DF | Adj. SS | Adj. MS | F-value | P-value | % influence |
|-------------------------------|----|---------|---------|---------|---------|-------------|
| Applied voltage (V)           | 3  | 0.695   | 0.231   | 9.62    | 0.048   | 60.35       |
| Duty cycle (%)                | 3  | 0.039   | 0.013   | 0.54    | 0.686   | 3.39        |
| Feed rate ( $\mu\text{m/s}$ ) | 3  | 0.359   | 0.119   | 4.97    | 0.110   | 31.18       |
| Frequency (Hz)                | 3  | 0.058   | 0.019   | 0.81    | 0.566   | 5.08        |
| Error                         | 3  | 0.072   | 0.024   |         |         |             |
| Total                         | 15 | 1.223   |         |         |         |             |

**Table 6** ANOVA for surface roughness

| Source                        | DF | Adj. SS | Adj. MS | F-value | P-value | % influence |
|-------------------------------|----|---------|---------|---------|---------|-------------|
| Applied voltage (V)           | 3  | 0.064   | 0.021   | 0.24    | 0.863   | 4.98        |
| Duty cycle (%)                | 3  | 0.485   | 0.162   | 1.84    | 0.315   | 38.18       |
| Feed rate ( $\mu\text{m/s}$ ) | 3  | 0.344   | 0.114   | 1.30    | 0.417   | 26.97       |
| Frequency (Hz)                | 3  | 0.380   | 0.127   | 1.44    | 0.386   | 29.87       |
| Error                         | 3  | 0.234   | 0.088   |         |         |             |
| Total                         | 15 | 1.537   |         |         |         |             |

### 3.2 Effect of Process Parameter on Dimensional Deviation

As shown in Fig. 8, the influence of the process parameters on dimensional deviation (DD) of ECMM process are plotted in main effect plots. From Fig. 8, it is clear that all the four parameters have considerable amount of effect on DD. It has been observed that applied voltage has huge impact on the dimensional deviation compared to other input parameters. Because, as the applied voltage increases, the

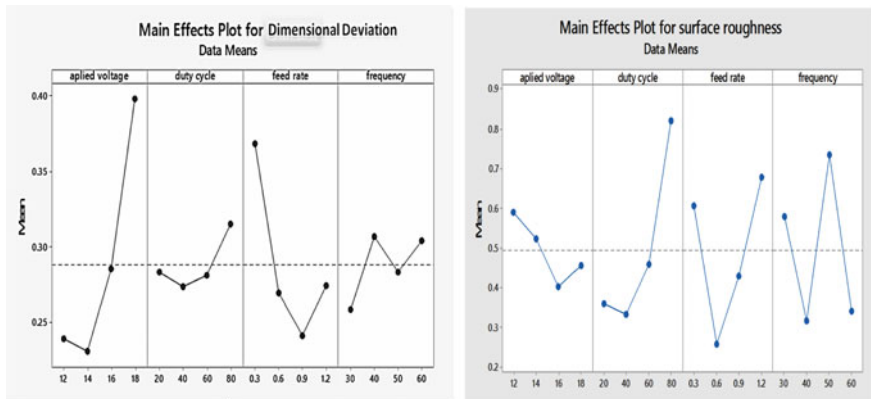


**Fig. 8** Main effect plots for means of dimensional deviation and surface roughness

electrolysis process gains more momentum towards machining and the peripheral surface of the tool also comes into machining which results in increase of hole diameter that in turn increase the dimensional deviation. As the voltage becomes very low, the energy required to break the titanium bonds is very less, so machining cannot be initiated. Hence, the applied voltage should be moderate for good dimensional accuracy of micro-holes in ECMM. Second variable that affects the dimensional deviation is feed rate, which can be observed from the main effect plots. As the feed rate increases, the amount of material to be removed from the titanium alloy increases with time. This will lead to rapid removal of the material and leads to poor dimensional accuracy. Duty cycle and frequency are not affecting this output response significantly.

### ***3.3 Effect of Process Parameters on Surface Roughness (SR)***

The influence of process parameters on surface roughness of titanium alloy (Ti6Al4V) are plotted in main effect plot and is shown in Fig. 8. From the figure, it has been clearly understood that duty cycle has more impact on SR. It has been cleared that SR increases with increase in duty cycle; this causes increase in pulse on time and decrease in pulse off time. Reducing pulse of time causes less time to remove the debris; hence, the improper surface finish is obtained. The pulse on time also increases material removal rate which resulted in higher surface roughness. SR first decreases and then increases by increasing tool feed rate ( $\mu\text{m/s}$ ). This is due to increasing feed rate up to optimum value, the results of SR are good, because fair amount of material is removed. Beyond this rapid removal causes irregular surfaces in the machining zone. Also, the feed rate influences the current density which causes the stray current effect significantly. Frequency is related to pulse on time and off time and depends on duty cycle and total time values. Hence, it has considerable effect on surface roughness based on experimental design values of pulse parameters.

## **4 Conclusions**

The current investigation focuses on the influence of process parameters of ECCM on dimensional deviation and surface roughness. Producing micro-holes on titanium-based alloy using ECMM process requires more voltage compared to commonly used metals and its alloys. The colour of the electrolyte is changed to yellow after machining due to titanium hydroxide  $[\text{Ti}(\text{OH})_4]$  and titanium chloride. Since the non-coated tool electrode is used, at higher voltage values the peripheral surface of the microtool comes in action during machining resulted in attaining the higher dimensional deviation values higher applied voltages. Non-contact surface roughness tester given the most accurate results, since the least count of the machine is in the range of less than 0.01 nm. From the results of ANOVA, it is concluded that applied voltage (60.35) has

more influence on dimensional deviation and duty cycle (38.18) has more influence on surface roughness.

**Acknowledgements** The authors would like to express gratitude towards **DST-FIST sponsored laboratories** of the Department of Manufacturing Engineering, Anna University, Chennai, for giving permission to use non-contact surface roughness testing machine facilities.

## References

1. Geethapriyan T, Kalaiichelvan K, Muthuramalingam T (2016) Multi performance optimization of electrochemical micro-machining process surface related parameters on machining Inconel 718 using Taguchi-grey relational analysis. *Metallurgia Italiana* 108(4):13–19
2. Bhattacharyya B, Malapati M, Munda J (2005) Experimental study on electrochemical micro-machining. *J Mater Process Technol* 169(3):485–492. <https://doi.org/10.1016/j.jmatprotec.2005.04.074>
3. Rama Rao S, Sravan CRM, Pandu Ranga V, Padmanabhan G (2009) Fuzzy logic-based forward modeling of electro chemical machining process. In: Proceedings on 2009 world congress on nature and biologically inspired computing, NABIC 2009, pp 1431–1435
4. Kalaimathi M, Venkatachalam G.S (2013) Experimental investigation on the electrochemical machining characteristics of monel 400 alloys and optimization of process parameters. *Jordon J Mech Ind Eng* 8(3):143–151. No. 3, ISSN 1995-6665
5. Dharmalingam S, Marimuthu P, Raja K (2017) Experimental investigation on electrochemical micro machining of Al-10%wt SiCp based on Taguchi design of experiments. *IRME* 7 (2014)
6. Sathiyamoorthy V, Sekar T, Suresh P, Vijayan R, Elango N (2015) Optimization of processing parameters in electrochemical machining of AISI 202 using response surface methodology. *J Eng Sci Technol* 10(6):780–789
7. Bhattacharyya B, Doloi B, Sridhar PS (2001) Electrochemical micro-machining: new possibilities for micro-manufacturing. *J Mater Process Technol* 113(1–3):301–305. [https://doi.org/10.1016/S0924-0136\(01\)00629-X](https://doi.org/10.1016/S0924-0136(01)00629-X)
8. Bhattacharyya B, Mitra S, Boro AK (2002) Electrochemical machining: new possibilities for micromachining. *Robot Comput-Integr Manuf* 18(3–4):283–289. [https://doi.org/10.1016/S0736-5845\(02\)00019-4](https://doi.org/10.1016/S0736-5845(02)00019-4)
9. Bhattacharyya B, Munda J (2003) Experimental investigation into electrochemical micromachining (EMM) process. *J Mater Process Technol* 140:287–291
10. Rajurkar KP, Zhu D, McGeough JA, Kozak J, De Silva A (1999) New developments in electro-chemical machining. *CIRP Ann Manuf Technol* 48(2):567–579. [https://doi.org/10.1016/S0007-8506\(07\)63235-1](https://doi.org/10.1016/S0007-8506(07)63235-1)
11. Senthil Kumar KL, Sivasubramanian R, Kalaiselvan K (2009) Selection of optimum parameters in non-conventional machining of metal matrix composite. *Portugaliae Electrochimica Acta* 27(4):477–486. <https://doi.org/10.4152/pea.200904477>
12. Sekar T, Marappan R (2008) Experimental investigations into the influencing parameters of electrochemical machining of AISI 202. *J Adv Manuf Syst* 07(02):337–343. <https://doi.org/10.1177/0218492313489696>
13. Kumar J, Khamba JS, Mohapatra SK (2008) An investigation into the machining characteristics of titanium using ultrasonic machining. *Int J Mach Mach Mater* 3(1/2):143. <https://doi.org/10.1504/IJMMM.2008.017631>
14. Dhobe SD, Doloi B, Bhattacharyya B (2011) Surface characteristics of ECMed titanium work samples for biomedical applications. *Int J Adv Manuf Technol* 55(1–4):177–188. <https://doi.org/10.1007/s00170-010-3040-5>

15. Blunt RT (2006). White Light Interferometry—a production worthy technique for measuring surface roughness on semiconductor wafers. Proc of CS MANTECH Conf 44(0):59–62. <https://doi.org/10.1017/CBO9781107256514>
16. Gao C, Qu N, He H, Meng L (2019) Double-pulsed wire electrochemical micro-machining of type-304 stainless steel. J Mater Process Technol 266: 381–387 (2019). <https://doi.org/10.1016/j.jmatprotec.2018.11.018>
17. Cole KM, Kirk DW, Singh CV, Thorpe SJ (2017) Optimizing electrochemical micromachining parameters for Zr-based bulk metallic glass. J Manuf Process 25:227–234. <https://doi.org/10.1016/j.jmapro.2016.11.015>
18. Meng L, Zeng Y, Zhu D (2017) Investigation on wire electrochemical micro machining of Ni-based metallic glass. Electrochim Acta 233:274–283. <https://doi.org/10.1016/j.electacta.2017.03.045>
19. A lecture notes on Micro Machining Processes by V.K. Jain, Mechanical Engineering Department, I.I.T Kanpur.
20. Kaplonek W, Lukianowicz C (2012) Coherence correlation interferometry in surface topography measurements. Recent interferometry applications in topography and astronomy, Ivan Padron, IntechOpen. <https://doi.org/10.5772/35059>